International Journal of Mass Spectrometry 283 (2009) 185–190

Contents lists available at ScienceDirect

International Journal of Mass Spectrometry

journal homepage: www.elsevier.com/locate/ijms

Collisional activation of ions by off-resonance irradiation in ion cyclotron resonance spectrometry

Seung Koo Shin*, Seung-Jin Han, Jongcheol Seo

FT-ICR Laboratory, Department of Chemistry, Pohang University of Science and Technology, San31 Hyojadong Namgu, Pohang, Kyungbuk, 790-784, Republic of Korea

ARTICLE INFO

Article history:
Received 30 November 2008
Received in revised form 15 March 2009
Accepted 19 March 2009
Available online 31 March 2009

Keywords:
Ion cyclotron resonance
Off-resonance burst irradiation
Time-resolved photodissociation

ABSTRACT

Collisional activation of ions in the ion cyclotron resonance (ICR) cell by short off-resonance burst irradiation (ORBI) was studied by time-resolved photodissociation of the *meta*-bromotoluene radical cation. Off-resonance chirp or single-frequency burst was applied for 2 ms to the probe ion in the presence of Ar buffer gas. The amount of internal energy imparted to the probe ion by collision under ORBI was precisely determined by time-resolved photodissociation spectroscopy. The rate of unimolecular dissociation of the probe ion following the photolysis at 532 nm was measured by monitoring the real-time appearance of the $C_7H_7^+$ product ion. The internal energy of the probe ion was extracted from the known rate-energy curve. To help understand the collisional activation of an ion under ORBI, we simulated the radial trajectory of the ion using Green's method. The calculated radial kinetic energy was converted to the collision energy in the center-of-mass frame, and the collision frequency was estimated by using a reactive hard-sphere collision model with an ion-induced dipole potential. Both experiments and trajectory simulations suggest that chirp irradiation leads to less collisional activation of ions than other waveforms.

1. Introduction

In Fourier-transform ion cyclotron resonance (FT-ICR) spectrometry [1–5], ions of interest are isolated in the ICR cell by radially ejecting all unwanted ions [6–16]. The radial ejection is typically accomplished by applying a radio frequency (rf) electric field in resonance with the effective cyclotron frequency of an ion to be removed [1,10–16]. Single-frequency bursts, frequency-swept chirps [2,17], tailored waveforms [18–25], and/or their combination are used to sweep out unwanted ions. However, the rf burst in resonance with one ion perturbs the trajectories of all other ions trapped in the ICR cell [19,26–29]. Thus, all remaining ions experience some translational agitation by off-resonance irradiation, which could lead to collisional activation of ions in the presence of buffer gas.

The on-resonance irradiation has been widely used in studies of ion-molecule reactions [30,31] as well as collision-induced dissociation (CID) [32–36], while the off-resonance irradiation [37] has been utilized in heating up large molecular ions [38–45]. Although the ion trajectory perturbed by off-resonance irradiation has been extensively studied by theory [29,46–49], the degree of internal excitation of ions by collision under such conditions has been rarely characterized by experiments. The effect of sustained off-resonance irradiation (SORI) on the collisional activation of ions has been recently reported by obtaining the fragmentation efficiency curve as a function of collision energy and applied frequency [50,51]. By contrast, the effect of transient off-resonance irradiation has not been well characterized. In a typical ICR experiment, a series of short rf bursts are applied to eject unwanted ion, however, their effects on the trajectory of an isolated ion are often neglected because each burst is not sustained for a long time. Nonetheless, the repetitive irradiation of a series of short rf bursts may yield a cumulative effect on the trajectory.

In this report, we examine the effect of off-resonance burst irradiation (ORBI) on the internal excitation of an ion. Because the degree of internal excitation is expected to be small, we use a sensitive internal energy probe. We have employed time-resolved photodissociation (TRPD) spectroscopy [52–57] to measure the rate of unimolecular dissociation of the bromotoluene radical cation. The unimolecular dissociation rate is a sensitive measure of an internal energy. Bromotoluene is one of the most well-characterized systems by experiments [54,55,58] and theory [59]. The bromotoluene radical cation dissociates to $C_7H_7^+$ upon a few eV internal excitation [54,55,58]. The lowest activation process leads to the benzyl cation via a series of hydrogen-migration intermediates [59], although the tropylium ion is thermodynamically more stable than the benzyl cation [60]. The rate-energy curve for the lowest activation process is available from the previous studies in our laboratory [55]. Thus, the internal energy can be precisely deter-

* Corresponding author. Tel.: +82 54 279 2123; fax: +82 54 279 3399.
E-mail address: skshin@postech.ac.kr (S.K. Shin).

1387-3806/$ – see front matter © 2009 Elsevier B.V. All rights reserved.
doi:10.1016/j.ijms.2009.03.008

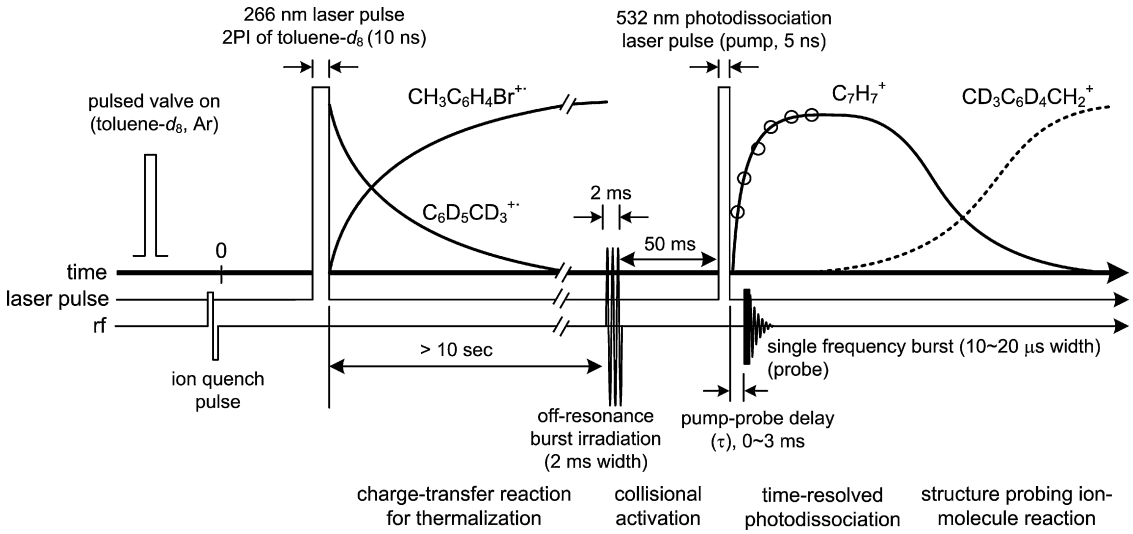

Fig. 1. Schematic of experimental procedures.

mined from the rate constant. Of the three geometric isomers, the *meta*-isomer is selected as a probe molecule because both the yield and dissociation rate best fit the 532-nm photolysis experiment in resolving the internal energy of ions excited by ORBI for 2 ms in the presence of Ar buffer gas.

To gain further insights into the translational agitation of an ion by ORBI, we calculate the radial trajectory of an ion in a cubic ICR cell by Green's method [61]. The radial kinetic energy of an ion in the laboratory frame is converted to the collision energy with Ar in the center-of-mass frame. The time-averaged collision energy is calculated by estimating the collision frequency using a reactive hard-sphere model with an ion-induced dipole potential [62].

2. Experimental

2.1. Time-resolved photodissociation

A 5-T FT-ICR setup for TRPD spectroscopy was previously described in detail [54]. The background pressure of an ICR chamber was typically below 9.0×10^{-10} torr after bakeout. Bromotoluene was leaked into the ICR cell through a leak valve (Varian, 951-5106) to reach a partial pressure of about 4×10^{-8} torr. Toluene-d_8 and Ar were admitted into the ICR cell through a pulsed valve. The partial pressures of toluene-d_8 and Ar were $\sim 2 \times 10^{-8}$ and 5×10^{-6} torr, respectively. The 266 nm output of a frequency-quadrupled Nd:YAG laser (Spectra-Physics, GCR-150) was used for photoionization and the 532 nm output of a frequency doubled Nd:YAG laser (Continuum, NY-8010) was used for photodissociation.

Experimental procedures are outlined in Fig. 1. One cycle of experiment begins with pulsing both toluene-d_8 and Ar followed by pulsing a quench voltage on trapping plates to refresh the ICR cell. Then, the toluene-d_8 radical cation ($C_6D_5CD_3^{+\bullet}$) is prepared by two-photon ionization (2PI) of toluene-d_8 (IE = 8.8276 eV) [63] at 266 nm. $C_6D_5CD_3^{+\bullet}$ undergoes exothermic charge-transfer reactions with neutral bromotoluene (IE = 8.73 eV) [58] for over 10 s with the rate constant of $k = 1.2 \times 10^{-9}$ cm^3 molecule^{-1} s^{-1} [54]. During this period, the bromotoluene radical cation ($CH_3C_6H_4Br^{+\bullet}$) is thermalized by degenerate charge-transfer reactions with neutral bromotoluene ($k = 1.8 \times 10^{-9}$ cm^3 molecule^{-1} s^{-1}) [54]. The direct 2PI of bromotoluene is not productive because of the fast predissociation in the S_1 state [55]. The space-charge effects [64] are minimized by lowering both the laser power and the partial pressure of toluene. After thermalization at 293 K, the bromotoluene radical cations (m/z = 170 and 172 Th) are irradiated for 2 ms by either a frequency-swept chirp in the mass range of m/z = 155–145 Th or a single-frequency burst at m/z = 155, 150, and 86 Th. The frequency range for m/z = 155–145 Th is selected to avoid overlaps with other nonlinear resonance frequencies from the quartic potential [65] and yet to be 9.7–17.3% off-resonant relative to the effective cyclotron frequency at m/z = 170 Th. The frequency at m/z = 86 Th is also tested because it is close to the second harmonics. After 50 ms delay, the parent ions are pumped by a 532 nm laser pulse and the appearance of the $C_7H_7^+$ product ion is probed with a 10–20 μs long rf excitation pulse as a function pump-probe delay on a μs time scale. Finally the structure of $C_7H_7^+$ is identified by the reaction of $C_7H_7^+$ with toluene-d_8.

One cycle of reaction events taking place in the ICR cell is summarized in Eqs. (1)–(5)

$$C_6D_5CD_3 + 2h\nu(266\,\text{nm}) \rightarrow C_6D_5CD_3^{+\bullet} + e^-\text{: photoionization} \quad (1)$$

$$C_6D_5CD_3^{+\bullet} + CH_3C_6H_4Br \rightarrow \mathit{CH}_3C_6H_4Br^{+\bullet} + C_6D_5CD_3\text{: charge transfer} \quad (2)$$

$$CH_3C_6H_4Br^{+\bullet} + CH_3C_6H_4\mathit{Br} \rightarrow CH_3C_6H_4\mathit{Br}^{+\bullet} + CH_3C_6H_4Br\text{ : thermalization} \quad (3)$$

$$CH_3C_6H_4\mathit{Br}^{+\bullet} + h\nu(532\,\text{nm}) \rightarrow C_7H_7^+ + \mathit{Br}^{\cdot}\text{: photodissociation} \quad (4)$$

$$C_7H_7^+ + C_6D_5CD_3 \rightarrow \mathit{CD}_3C_6D_4CH_2^+ + C_6H_5D\text{ : structure identification} \quad (5)$$

For the time-resolved ion detection [54], a single-frequency burst is applied at the effective cyclotron frequency of $C_7H_7^+$ for 10–20 μs with 44-V peak-to-peak amplitude and the ICR transient is acquired for 8.192 ms. For collisional activation of ions, the off-resonance rf burst is applied for 2 ms with 44-V peak-to-peak amplitude.

To extract the internal energy of an ion, we iteratively fit the TRPD yield data to the ICR signal equation convoluted with a truncated Boltzmann distribution [66–69]. The time-resolved ICR signal equation is given in Eqs. (6) and (7) [54]

$$S(t) = C(t + \Delta - t_0)\left(1 - \frac{1 - \exp^{-k(t+\Delta-t_0)}}{k(t + \Delta - t_0)}\right) \quad \text{for } t \le t_0 \le t + \Delta \tag{6}$$

$$S(t) = C\Delta\left(1 - \exp^{-k(t-t_0)}\frac{1 - \exp^{-k\Delta}}{k\Delta}\right) \quad \text{for } t_0 \le t \tag{7}$$

where $S(t)$ is the product ion signal, C is the proportionality constant, Δ is the pulse width of an rf detection burst, and k is the unimolecular dissociation rate constant. The pump laser is fired at t_0, while the rf detection burst is scanned before and after the pump laser. The precise timing of the beginning of the rf detection burst with respect to the pump laser is monitored by using a fast photodiode with a 200-MHz digital oscilloscope (LeCroy 9304M).

2.2. Trajectory calculations and collision dynamics

In a cubic ICR cell of length a (50.8 mm) and trapping potential V, the radial equation of motion of an ion with mass m and charge q under a homogeneous magnetic field **B** directed along the z-axis and a dipolar rf excitation force field along the x-axis is given to the first order in Eq. (8) [65]

$$\ddot{R} + i\omega_c\dot{R} - \frac{\omega_z^2}{2}R = -\frac{qb_0}{ma}F(t) \tag{8}$$

where $R(t) = x(t) + iy(t)$, ω_c ($= qB/m$) is the cyclotron frequency ω_z ($= \sqrt{4qa_0V/ma^2}$) is the axial oscillation frequency, and $F(t)$ is an arbitrary rf excitation function. For a cubic cell, $a_0 = 1.386865$ and $b_0 = 1.4433$ [65]. Assuming a linear response, the inhomogeneous part of differential equation can be expressed as a sum of individual impulse functions by applying superposition principle [61]. Green's method is useful to find a solution for linear, inhomogeneous differential equations with the initial conditions of $R(0) = 0$ and $\dot{R}(0) = 0$.

$$R(t) = \int_0^t F(t') \cdot G(t, t')\ dt' \tag{9}$$

where

$$G(t, t') \equiv \frac{iqb_0}{ma(\omega_+ - \omega_-)}(\exp -i\omega_-(t - t') - \exp -i\omega_+(t - t')) \tag{10}$$

and

$$\omega_\pm = \frac{\omega_c}{2}\left(1 \pm \sqrt{1 - \frac{2\omega_z^2}{\omega_c^2}}\right) \tag{11}$$

The Green's function $G(t, t')$, which is a solution for the differential equation of an infinitesimal element of the inhomogeneous part, already contains the initial conditions. Therefore, the general solution, expressed by the integral of $F(t')\cdot G(t, t')$, automatically contains the initial conditions for any rf excitation function $F(t)$. The radial trajectory $R(t)$ is obtained by numerical integration of $F(t')\cdot G(t, t')$. The derivative $\dot{R}(t)$ is also evaluated numerically to give the kinetic energy of an ion Eq. (12)

$$E_{tr}(t) = \frac{1}{2}m|\dot{R}(t)|^2 \tag{12}$$

The kinetic energy in the laboratory frame is converted to the collision energy with Ar in the center-of-mass frame Eq. (13)

$$E_{cm}(t) = \frac{m_{Ar}}{m + m_{Ar}}E_{tr}(t) = \frac{m_{Ar}}{m + m_{Ar}}\frac{1}{2}m|\dot{R}(t)|^2 = \frac{1}{2}\mu|\dot{R}(t)|^2 \tag{13}$$

where μ is the reduced mass. To compare with experiments, the collision frequency is estimated by adopting a reactive hard-sphere collision model with an ion-induced dipole potential [62]. The effective collision cross-section $\sigma(v)$ is given in Eqs. (14) and (15)

$$\sigma(v) = \frac{2\pi q}{v}\sqrt{\frac{\alpha}{\mu}} \quad \text{for } v \le \frac{q}{d^2}\sqrt{\frac{\alpha}{\mu}} \tag{14}$$

$$\sigma(v) = \pi d^2\left(1 + \frac{\alpha q^2}{\mu v^2 d^4}\right) \quad \text{for } v \ge \frac{q}{d^2}\sqrt{\frac{\alpha}{\mu}} \tag{15}$$

where v is the relative velocity, α is the polarizability of Ar (1.6411 Å^3) [70], and d ($= r_{ion} + r_{Ar} = 3.9$ Å + 1.7 Å) is the effective hard-sphere radius. For a given ion velocity, $v_i = |\dot{R}(t)|$, the collision frequency with Ar having a Maxwell–Boltzmann velocity distribution is expressed as Eq. (16)

$$Z(v_i) = n_{Ar}\sqrt{\frac{m_{Ar}}{2\pi k_B T}}\frac{1}{v_i}\int_0^\infty \sigma(v)v^2(\exp^{-m_{Ar}(v-v_i)^2/2k_BT} - \exp^{-m_{Ar}(v+v_i)^2/2k_BT})\ dv \tag{16}$$

where n_{Ar} is the number density of Ar. The probability of multiple collisions is estimated by the Poisson distribution Eq. (17) [71]

$$P_m(t) = \frac{e^{-Zt}(Zt)^m}{m!} \tag{17}$$

3. Results and discussion

3.1. Time-resolved photodissociation of ions perturbed by off-resonance burst irradiation

The TRPD spectra presented in Fig. 2 show the time-resolved appearance of the $C_7H_7^+$ product ion from 532-nm photodissociation of the bromotoluene radical cation. The time-zero intercept represents the relative yield of two-photon dissociation (2PD) and the initial slope corresponds to the rate of one-photon dissociation (1PD). The parent ion thermalized at 293 K with no rf irradiation dissociates at the rate of $3700 \pm 200\ s^{-1}$ with an internal energy of 2.43 eV (one photon energy at 532 nm plus thermal internal energy at 293 K) [55]. After 2-ms long chirp irradiation at $\omega_e/2\pi = 495\,064$–$529\,217$ Hz ($\omega_e/\omega_c = 1.097$–$1.173$) covering the mass range of $m/z = 155$–145 Th, both the time-zero intercept and initial slope increase significantly. Signal analysis using the rate-energy curve for the *meta*-bromotoluene radical cation [54] suggests that the internal energy of the parent ion increases by ~60 meV from the thermal value at 293 K. The 2-ms long single-frequency burst irradiation at the median m/z of 150 Th ($\omega_e/2\pi = 511\,572$ Hz, $\omega_e/\omega_c = 1.134$) also produces similar increases in both the intercept and slope, indicating the same degree of internal excitation. To compare with chirp irradiation, we varied the burst frequency as shown in Fig. 2b, one at 1.097 ω_c corresponding to $m/z = 155$ and the other at 1.977 ω_c corresponding to $m/z = 86$. The rate-energy curve suggests that the internal energy increases by ~80 and ~20 meV from the thermal value after burst irradiation at $m/z = 155$ and 86, respectively. Apparently, short ORBI perturbs the radial trajectories of ions in the ICR cell to induce collisional activation of ions in the presence of buffer gas.

3.2. Kinetic energy modulation by off-resonance burst irradiation

To illustrate the perturbation of radial kinetic energy of an ion by ORBI, we simulate the trajectory of an ion at $m/z = 170$ ($\omega_c/2\pi = 451\,220$ Hz) in a 5 T magnetic field strength and numerically calculate the radial kinetic energy as a function of applied frequency (ω_e/ω_c) and irradiation time. The ion is initially at rest in the center of the ICR cell ($R(0) = 0$ and $\dot{R}(0) = 0$) and irradiated by a dipolar rf electric

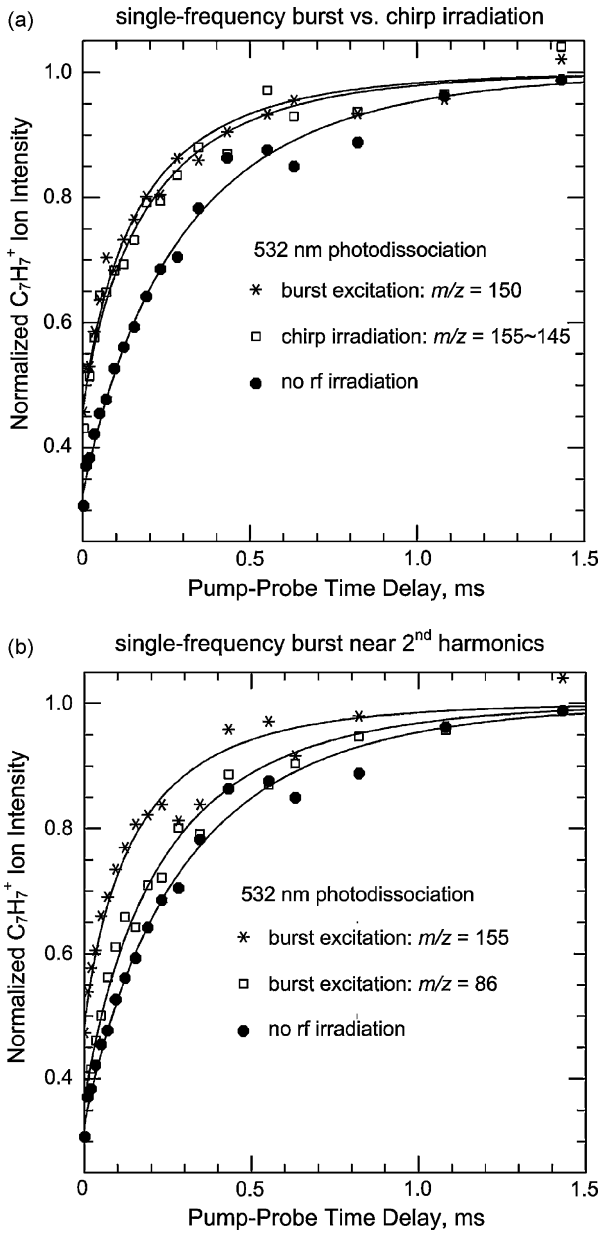

Fig. 2. The TRPD spectra of the *m*-bromotoluene radical cation at 532 nm with a laser power of ~5 mJ per pulse: (a) the appearance of the $C_7H_7^+$ product ion from 532-nm photolysis of the parent ion under no rf irradiation (●), chirp irradiation in the mass range of m/z = 155–145 Th (□), and burst irradiation at m/z = 150 Th (*); (b) the appearance of the $C_7H_7^+$ product ion from 532-nm photolysis of the parent ion under no rf irradiation (●), and burst irradiation at m/z = 86 Th (□) and at m/z = 155 Th (*). The duration of burst is 2 ms. The line is a fit to the convoluted signal equation.

field along the *x*-axis with peak-to-peak amplitude of 34 V. The ion kinetic energy oscillates sinusoidally with irradiation time as shown in Fig. 3. The most prominent modulation is due to the most slowly varying difference-frequency ($\omega_e - \omega_+$) component. The fine modulation on top of the large-amplitude difference-frequency modulation is due to the sum-frequency ($\omega_e + \omega_+$) component. The modulation of the second harmonic ($2\omega_e$) component is not resolved. The maximum kinetic energy decreases as the ratio of off-resonance frequency to cyclotron frequency (ω_e/ω_c) increases. The well-known equation for the maximum kinetic energy achieved by SORI is in fact the zeroth-order approximation, where the kinetic energy is proportional to the square of applied rf amplitude and inversely proportional to the square of difference frequency ($\omega_e - \omega_+$).

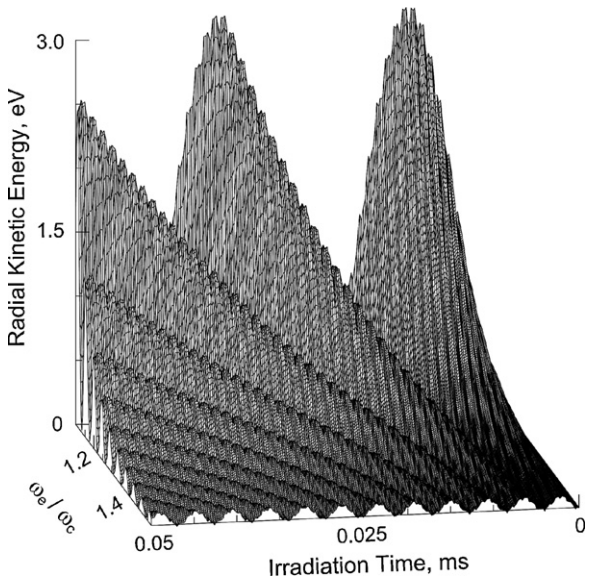

Fig. 3. The modulation of kinetic energy (E_{tr}) of an ion at m/z = 170 ($\omega_c/2\pi$ = 451,220 Hz) as a function of ω_e/ω_c and irradiation time with 34-V peak-to-peak amplitude. The large-amplitude modulation is due to the slowly varying difference-frequency ($\omega_e - \omega_+$) component, while the fine modulation on top of the difference-frequency modulation is due to the sum-frequency ($\omega_e + \omega_+$) component.

To more closely examine the effects of different waveforms on the translational agitation of the ion at m/z = 170, we calculate the kinetic energy modulated by either a single-frequency burst at m/z = 155, 150, and 145, or a superposition of three frequencies, or a frequency-swept chirp. After converting into the collision energy, the modulation of collision energy is depicted in Fig. 4 as a function of irradiation time of different waveforms. Under single-frequency burst irradiation, the collision energy oscillates sinusoidally with the difference frequency ($\omega_e - \omega_+$) and the maximum collision energy is proportional to $1/(\omega_e - \omega_+)^2$. When the superposition waveform is applied, the collision energy fluctuates with much higher amplitude than the sum of three amplitudes from single-frequency bursts due to interferences. By contrast, the chirp waveform results in much reduced modulation of collision energy with the maximum collision energy almost identical to that achieved by single-frequency burst at the median m/z = 150.

Assuming the present experimental condition leads to the time-averaged collision energy of 140, 72 and 42 meV for ORBI at m/z = 155, 150 and 145 Th, respectively, with the average collision frequency of 140, 70 and 48 s^{-1}, respectively. The ratio of average collision energy is 3.33:1.71:1.00 and that of average collision frequency is 2.91:1.46:1.00 for ORBI at m/z = 155, 150 and 145 Th, respectively. Both ratios are close to the ratio of 3.17:1.67:1.00 for $1/(\omega_e - \omega_c)^2$ at m/z = 155, 150 and 145 Th, respectively. The probability of collision with Ar during 2-ms ORBI at m/z = 155, 150, and 145 Th is calculated to be 0.21, 0.12, and 0.09 for single collision and 0.03, 0.009, and 0.004 for double collision, respectively. Provided that the parent ion undergoes, on average, less than one collision during ORBI and the translational-to-vibrational energy-transfer efficiency is not unity, the amount of increase in internal energy by 80 and 60 meV due to ORBI at m/z = 155 and 150 Th is in reasonable agreement with the calculated average collision energy of 140 and 70 meV, respectively.

3.3. Sustained off-resonance irradiation at m/z = 155 and 145

Under the single collision condition, the net amount of internal energy imparted by ORBI is limited by the maximum collision

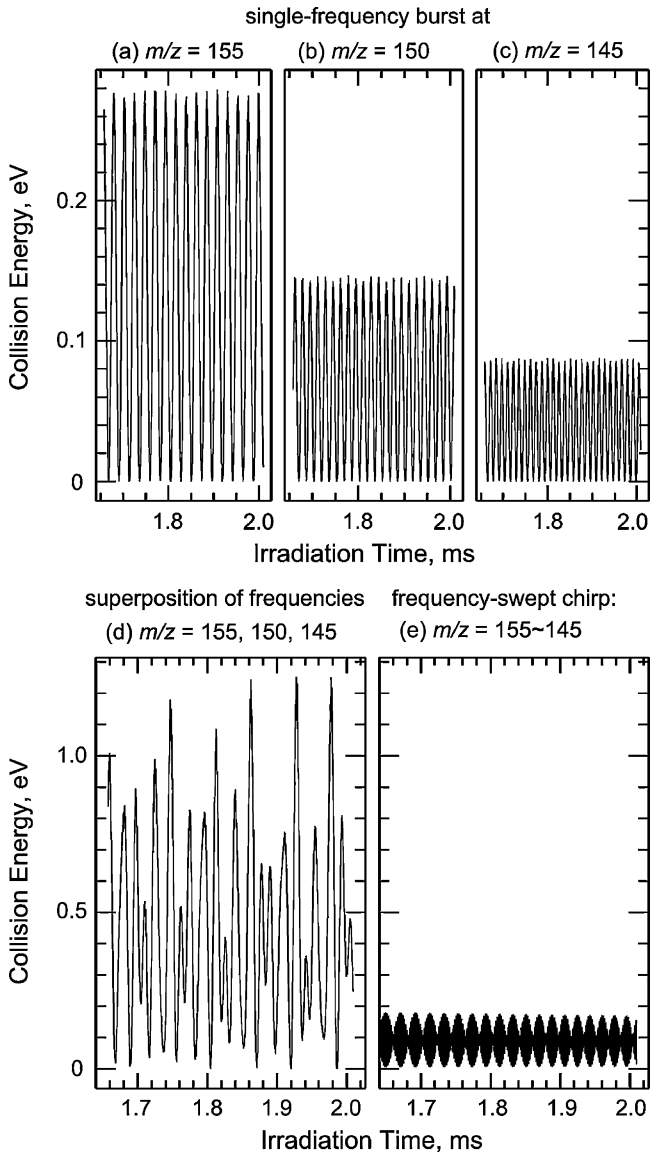

Fig. 4. The modulation of collision energy (E_{cm}) of an ion at $m/z = 170$ with Ar as a function of burst duration with 44 V peak-to-peak amplitude: (a) single-frequency burst at $m/z = 155$ Th ($\omega_e/\omega_c = 1.097$); (b) single-frequency burst at $m/z = 150$ Th ($\omega_e/\omega_c = 1.134$); (c) single-frequency burst at $m/z = 145$ Th ($\omega_e/\omega_c = 1.173$); (d) a superposition of frequencies at $m/z = 155$, 150, and 145 Th; (e) frequency-swept chirp covering the mass range of $m/z = 155$–145 Th. The step size of chirp is 17 Hz and the duration of each chirp step is 1 μs.

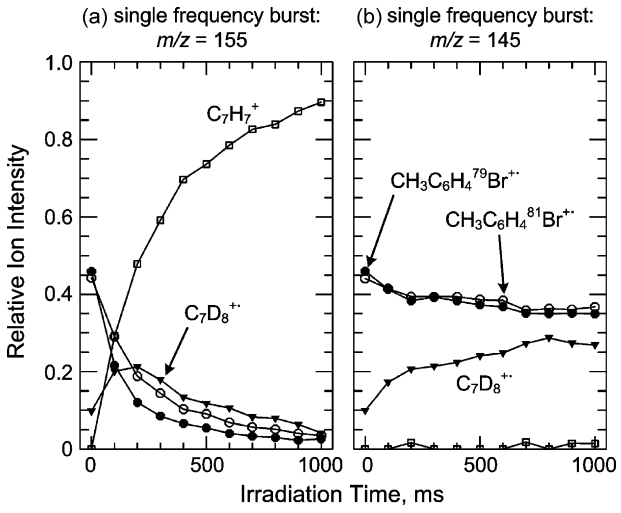

Fig. 5. Temporal variations of ion-molecule reactions taking place under sustained off-resonance irradiation of single-frequency burst at (a) $m/z = 155$ and (b) $m/z = 145$. The peak-to-peak amplitude is 44 V. At time zero, the relative abundance of the bromotoluene radical cation ($CH_3C_6H_4{}^{79/81}Br^{+\bullet}$) is 90% and that of the toluene-d_8 radical cation ($C_7D_8{}^{+\bullet}$) is 10%. The solid circle (●) represents $CH_3C_6H_4{}^{79}Br^{+\bullet}$ at $m/z = 170$, the open circle (○) denotes $CH_3C_6H_4{}^{81}Br^{+\bullet}$ at $m/z = 172$, the solid triangle (▼) represents $C_6D_5CD_3{}^{+\bullet}$ at $m/z = 100$, and the open square (□) is $C_7H_7{}^+$ at $m/z = 91$. The charge-transfer from $CH_3C_6H_4{}^{79/81}Br^{+\bullet+}$ to toluene-d_8 to yield $C_6D_5CD_3{}^{+\bullet}$ is endothermic by 0.10 eV, whereas the dissociation of $CH_3C_6H_4{}^{79/81}Br^{+\bullet+}$ to the benzyl cation ($C_6H_5CH_2{}^+$) requires an activation energy of 1.80 eV.

energy which is proportional to $1/(\omega_e - \omega_c)^2$. So ORBI at $m/z = 155$ can impart more energy into the internal degrees of freedom than ORBI at $m/z = 145$ by a factor of 3.17 in theory. Under the multiple collision condition, however, the net amount of internal energy imparted by SORI is proportional to the product of average collision energy and average collision frequency, thus becoming roughly proportional to the square of $1/(\omega_e - \omega_c)^2$.

To illustrate this significant difference between single-collision ORBI and multiple-collision SORI, we apply SORI to the bromotoluene radical cation. The bromotoluene radical cation can undergo two different reactions upon collisional activation depending on available internal energy. One is the charge-transfer reaction with toluene-d_8 to yield the toluene-d_8 radical cation (the reverse of Eq. (2)), which is endothermic by 0.1 eV [54], and the other is the unimolecular dissociation to $C_7H_7{}^+$, which requires activation energy of 1.80 eV [55]. We observe the reaction profile as a function of irradiation time of single-frequency burst at $m/z = 155$ and 145 Th. Temporal variations of ion intensities are plotted in Fig. 5 as a function of irradiation time. When the $m/z = 155$ burst is applied, the bromotoluene radical cation undergoes charge-transfer reactions with toluene-d_8 as well as unimolecular dissociation. The $m/z = 170$ Th isomer ($CH_3C_6H_4{}^{79}Br^{+\bullet}$) reacts away faster than the $m/z = 172$ Th isomer ($CH_3C_6H_4{}^{81}Br^{+\bullet}$) due to close proximity in frequency to the burst frequency at $m/z = 155$ Th. The toluene-d_8 radical cation ($C_7D_8{}^{+\bullet}$) is continually converted back to the bromotoluene radical cation by exothermic reaction with neutral bromotoluene as given in Eq. (2). As the bromotoluene radical cation is gradually depleted to $C_7H_7{}^+$, the toluene-d_8 radical cation is also depleted. All $C_7H_7{}^+$ product ions react with toluene-d_8 to yield $CD_3C_6D_4CH_2{}^+$, confirming the benzyl structure for $C_7H_7{}^+$. On the other hand, when the $m/z = 145$ burst is applied, no unimolecular dissociation product $C_7H_7{}^+$ is observed, but the toluene-d_8 radical cation reaches the steady state with the bromotoluene radical cation upon sustained irradiation. This clear difference in product branching between the two SORIs at $m/z = 155$ and 145 demonstrates the effects of multiple collisions on collisional activation of ions. Unlike single-collision conditions, the product of average collision energy and average collision frequency determines the degree of translation-to-vibrational energy transfer. Although the ratio of average collision energy and average collision frequency is 3.33 and 2.91 for the $m/z = 155$ burst irradiation with respect to the $m/z = 145$ burst irradiation, respectively, a value of 9.7 for their product is close to a value of 10.0 for the square of the ratio of $1/(\omega_e - \omega_c)^2$. In comparison, the ratio of activation energy for unimolecular dissociation to enthalpy for charge-transfer reaction is 18. It seems that a small difference in off-resonance frequency can make a big difference in product branching because multiple collisions taking place under SORI lead to climb up the energy ladder more frequently with a larger step.

4. Conclusion

The least perturbing waveform for ejecting ions out of the ICR cell is obviously the frequency-sweeping chirp rather than a series

of single-frequency bursts or their superposition waveform. As expected, a single-frequency burst results in a sinusoidal oscillation of kinetic energy at the beat frequency, a superposition waveform leads to a large amplitude fluctuation of kinetic energy due to interference, while the chirp yields a small-amplitude oscillation due to continually varying discrete frequencies without interference. Ions under transient off-resonance burst irradiation mostly undergo a single collision, thus the average collision energy determines the degree of internal excitation by collision. By contrast, ions under sustained off-resonance irradiation undergo multiple collisions, thus the product of average collision energy and average collision frequency determines the degree of internal excitation.

Acknowledgment

We acknowledge the support from the Functional Proteomics Center (Grant No. FPR08A1-040).

References

[1] M.B. Comisarow, A.G. Marshall, Chem. Phys. Lett. 25 (1974) 282.
[2] M.B. Comisarow, A.G. Marshall, Chem. Phys. Lett. 26 (1974) 489.
[3] K.P. Wanczek, Int. J. Mass Spectrom. Ion Process. 95 (1989) 1.
[4] A.G. Marshall, L. Schweikhard, Int. J. Mass Spectrom. Ion Process. 118 (1992) 37.
[5] C.W. Ross, S.H. Guan, P.B. Grosshans, T.L. Ricca, A.G. Marshall, J. Am. Chem. Soc. 115 (1993) 7854.
[6] S.K. Shin, S.J. Han, J. Am. Soc. Mass Spectrom. 8 (1997) 86.
[7] R.T. McIver Jr., Rev. Sci. Instrum. 41 (1970) 555.
[8] T.B. McMahon, J.L. Beauchamp, Rev. Sci. Instrum. 43 (1972) 509.
[9] S.A. Hofstadler, D.A. Laude, Anal. Chem. 63 (1991) 2001.
[10] S.C. Beu, D.A. Laude, Anal. Chem. 64 (1992) 177.
[11] W.W. Yin, M. Wang, A.G. Marshall, E.B. Ledford, J. Am. Soc. Mass Spectrom. 3 (1992) 188.
[12] Z.Q. Guan, S.A. Hofstadler, D.A. Laude, Anal. Chem. 65 (1993) 1588.
[13] R. Chen, A.G. Marshall, Int. J. Mass Spectrom. Ion Process. 133 (1994) 29.
[14] J.A. Marto, A.G. Marshall, L. Schweikhard, Int. J. Mass Spectrom. Ion Process. 137 (1994) 9.
[15] V.H. Vartanian, J.S. Anderson, D.A. Laude, Mass Spectrom. Rev. 14 (1995) 1.
[16] V.H. Vartanian, D.A. Laude, Anal. Chem. 68 (1996) 1321.
[17] A.J. Noest, C.W.F. Kort, Comp. Chem. 7 (1983) 81.
[18] T.-C.L. Wang, T.L. Ricca, A.G. Marshall, Anal. Chem. 58 (1986) 2935.
[19] L. Chen, A.G. Marshall, Int. J. Mass Spectrom. Ion Process. 79 (1987) 115.
[20] C.D. Hanson, M.E. Castro, E.L. Kerley, D.H. Russell, Anal. Chem. 62 (1990) 1352.
[21] S.H. Guan, J. Chem. Phys. 93 (1990) 8442.
[22] P.B. Grosshans, A.G. Marshall, Anal. Chem. 63 (1991) 2057.
[23] K.A. Boering, J. Rolfe, J.I. Brauman, Rapid Commun. Mass Spectrom. 6 (1992) 303.
[24] S. Haebel, T. Gaumann, Int. J. Mass Spectrom. Ion Process. 144 (1995) 139.
[25] S.H. Guan, A.G. Marshall, Int. J. Mass Spectrom. Ion Process. 158 (1996) 5.
[26] M.D. Wang, A.G. Marshall, Anal. Chem. 62 (1990) 515.
[27] A.J.R. Heck, L.J. Dekoning, F.A. Pinkse, N.M.M. Nibbering, Rapid Comm. Mass Spectrom. 5 (1991) 406.
[28] D.E. Riegner, D.A. Laude, Int. J. Mass Spectrom. Ion Process. 120 (1992) 103.
[29] X.Z. Xiang, A.G. Marshall, J. Am. Soc. Mass Spectrom. 5 (1994) 807.
[30] L.R. Anders, J.L. Beauchamp, R.C. Dunbar, J.D. Baldeschwieler, J. Chem. Phys. 45 (1966) 1062.
[31] J.L. Beauchamp, Annu. Rev. Phys. Chem. 22 (1971) 527.
[32] R.B. Cody, R.C. Burnier, C.J. Cassady, B.S. Freiser, Anal. Chem. 54 (1982) 2225.
[33] R.B. Cody, B.S. Freiser, Anal. Chem. 54 (1982) 1431.
[34] R.B. Cody, R.C. Burnier, B.S. Freiser, Anal. Chem. 54 (1982) 96.
[35] R.B. Cody, B.S. Freiser, Int. J. Mass Spectrom. Ion Process. 41 (1982) 199.
[36] R.L. White, C.L. Wilkins, Anal. Chem. 54 (1982) 2211.
[37] J.W. Gauthier, T.R. Trautman, D.B. Jacobson, Anal. Chim. Acta 246 (1991) 211.
[38] Y.Q. Huang, B.S. Freiser, J. Am. Chem. Soc. 115 (1993) 737.
[39] S.A. Hofstadler, J.H. Wahl, R. Bakhtiar, G.A. Anderson, J.E. Bruce, R.D. Smith, J. Am. Soc. Mass Spectrom. 5 (1994) 894.
[40] M.W. Senko, J.P. Speir, F.W. Mclafferty, Anal. Chem. 66 (1994) 2801.
[41] Y.L. Huang, L. Pasatolic, S.H. Guan, A.G. Marshall, Anal. Chem. 66 (1994) 4385.
[42] Q.Y. Wu, S. Vanorden, X.H. Cheng, R. Bakhtiar, R.D. Smith, Anal. Chem. 67 (1995) 2498.
[43] R.L. Hettich, E.A. Stemmler, Rapid Commun. Mass Spectrom. 10 (1996) 321.
[44] T. Solouki, L. Pasatolic, G.S. Jackson, S.G. Guan, A.G. Marshall, Anal. Chem. 68 (1996) 3718.
[45] V.C.M. Dale, J.P. Speir, G.H. Kruppa, C.C. Stacey, M. Mann, M. Wilm, Biochem. Soc. Trans. 24 (1996) 943.
[46] C.D. Hanson, E.L. Kerley, M.E. Castro, D.H. Russell, Anal. Chem. 61 (1989) 2040.
[47] C.D. Hanson, M.E. Castro, D.H. Russell, Anal. Chem. 61 (1989) 2130.
[48] B.A. Hearn, C.H. Watson, G. Baykut, J.R. Eyler, Int. J. Mass Spectrom. Ion Process. 95 (1990) 299.
[49] M. Wang, A.G. Marshall, Int. J. Mass Spectrom. Ion Process. 100 (1990) 323.
[50] J. Laskin, M. Byrd, J. Futrell, Int. J. Mass Spectrom. 195/196 (2000) 285.
[51] J. Laskin, J. Futrell, J. Phys. Chem. A 104 (2000) 5484.
[52] R.C. Dunbar, J. Phys. Chem. 91 (1987) 2801.
[53] R.C. Dunbar, C. Lifshitz, J. Chem. Phys. 94 (1991) 3542.
[54] S.K. Shin, S.-J. Han, B. Kim, Int. J. Mass Spectrom. Ion Process. 158 (1996) 345.
[55] B. Kim, S.K. Shin, J. Chem. Phys. 106 (1997) 1411.
[56] S.K. Shin, B. Kim, R.L. Jarek, S.-J. Han, Bull. Korean Chem. Soc. 23 (2002) 267.
[57] B. Kim, S.K. Shin, J. Phys. Chem. A 106 (2002) 9918.
[58] S. Olesik, T. Baer, J.C. Morrow, J.J. Ridal, J. Buschek, J.L. Holmes, Org. Mass Spectrom. 24 (1989) 1008.
[59] J.C. Choe, Int. J. Mass Spectrom. 278 (2008) 50.
[60] S.K. Shin, Chem. Phys. Lett. 280 (1997) 260.
[61] J.B. Marion, Classical Dynamics of Particles and Systems, 2nd ed., Academic Press, New York, 1970.
[62] E.F. Greene, A. Kuppermann, J. Chem. Educ. 45 (1968) 361.
[63] K.T. Lu, G.C. Eiden, J.C. Weisshaar, J. Phys. Chem. 96 (1992) 9742.
[64] S.-J. Han, S.K. Shin, J. Am. Soc. Mass Spectrom. 8 (1997) 319.
[65] S.K. Shin, S.-J. Han, Int. J. Mass Spectrom. Ion Process. 153 (1996) 87.
[66] R.C. Dunbar, J. Chem. Phys. 91 (1989) 6080.
[67] J.D. Faulk, R.C. Dunbar, C. Lifshitz, J. Am. Chem. Soc. 112 (1990) 7893.
[68] R.C. Dunbar, J. Chem. Phys. 95 (1991) 2537.
[69] R.C. Dunbar, J. Phys. Chem. 98 (1994) 8705.
[70] R.C. Weast, CRC Handbook of Chemistry and Physics, 1st Student ed., CRC Press, Boca Raton, 1988.
[71] M.S. Kim, Int. J. Mass Spectrom. Ion Phys. 50 (1983) 189.